ИНСТИТУТ ЯДЕРНОЙ ФИЗИКИ СО АН СССР

Boris V. Chirikov

PATTERNS IN CHAOS

PREPRINT 90-109

НОВОСИБИРСК

Patterns in Chaos*)

Boris V. Chirikov

Institute of Nuclear Physics,
630090, Novosibirsk, USSR

ABSTRACT

Classification of chaotic patterns in classical Hamiltonian systems is given as a series of levels with increasing disorder. Overview of critical phenomena in Hamiltonian dynamics is presented, including the renormalization chaos, based upon the fairly simple resonant theory. First estimates for the critical structure and related statistical anomalies in arbitrary dimensions are discussed.

---

*) Revised text of the lectures given at the International School on Order, Chaos and Patterns, Como, 1990.

© *Институт ядерной физики СО АН СССР*

CONTENTS

INTRODUCTION

The main idea I would like to expose here is inexhaustible diversity and richness of the dynamical chaos whatever description you choose: trajectories, statistics or, recently, renormalization. The importance of this relatively new phenomenon — the dynamical chaos — is in that it presents, even in very simple models to be discussed below, the surprising complexity of the structures and evolution characteristic for a broad range of processes in nature including the highest levels of its organization. Moreover, dynamical chaos is the only stationary source of any new information and, hence, a necessary part of any creative activity, the science including. This is a direct implication of the Alekseev — Brudno theorem and Kolmogorov's development in the information theory (see, e. g., Refs [1, 2]). The chaos is not always that bad!

Below I restrict myself to the classical mechanics only. The so-called «quantum chaos» is another story (see, e. g., Refs [3, 4]). Let me just mention that apart from very exotic examples there is no «true» chaos in quantum mechanics contrary to a common belief. On the other hand, the inavoidable statistical element of quantum mechanics related to the measurement is very likely assotiated with the same classical chaos in the measuring device.

With a bit of imagination and fantasy one may even conjecture that any macroscopic event in this World, which formally is a result of some quantum «measurement», would be impossible without chaos.

Also, I am not going to consider any dissipative models (very important in practical applications) because they are not as fundamental as Hamiltonian systems. Besides, strictly speaking, the dissipative systems are not purely dynamical as the dissipation is inevitable related to some noise.

In what follows I take a physicist's approach to the problem, that is my presentation will be based on a simple (sometimes even qualitative) theory combined with the results of extensive numerical (computer) experiments. For a good physical overview of nonlinear dynamics and chaos, see books [5, 6].

The principal concept of such a theory is the nonlinear resonance whose quite familiar by now phase space picture is depicted, e. g., in Fig. 4 below. Essential part of this resonance structure is a pair of periodic orbits, the most important being unstable one as it gives rise to the separatrix and, under almost any perturbation, to a chaotic layer around. This is precisely the place where chaos is dawning.

Again, I have to restrict myself to a simpler case of strong nonlinearity which does not vanish with perturbation. A very interesting weakly nonlinear resonance will be briefly mentioned in Section 1.2 below.

The paper is organized as follows. In the next Section 1 simple models are described currently extensively used in the studies of nonlinear phenomena and chaos. They well represent the whole spectrum of complexity classified in Section 2. The main Sections 3 and 4 are devoted to a detailed description of the so-called critical phenomena in dynamics which reveal the most complicated behaviour presently known.

1. SIMPLE MODELS

First, let us consider a number of simple models currently very popular in the studies of dynamical chaos. Most of them are specified by some mappings, or maps, rather than by differential equations. This considerably simplifies both the theoretical analysis and, especially, the computer experiments.

In conservative Hamiltonian systems the chaos requires, at least, two freedoms. Then, the corresponding so-called Poincaré map is two-dimensional.

1.1. Strong nonlinearity [7]. Below we shall consider $2D$ maps of the following form:

$$\bar{y}=y+f(x)\,; \qquad \bar{x}=x+g(\bar{y})\,. \tag{1.1}$$

This map is area-preserving, or canonical, which corresponds to the Hamiltonian nature of the model. Function $f(x)$, periodic in x, describes a perturbation usually assumed to be small. Hence, y is the unperturbed motion integral. Function $g(y)$, even linear (see Eq. (1.6) below), represents the nonlinearity of x oscillation.

The simplest example of an analytic perturbation is given by

$$f(x)=K\cdot\sin x\,. \tag{1.2}$$

We shall consider also a smooth perturbation specified by the Fourier series

$$f(x)=\sum_m f_m e^{imx}\,; \qquad f_m\sim K|m|^{-\beta}, \tag{1.3}$$

where β is the smoothness parameter. The term «smooth» means actually «not smooth enough». For $\beta=2$, for example, function $f(x)$ is continuous but the first derivative is discontinuous.

I mention two particular forms of nonlinearity. The first one

$$g(y)=\lambda\cdot\ln|y| \tag{1.4a}$$

models the motion near separatrix of a nonlinear resonance, so that map (1.1) with this nonlinearity and perturbation (1.2) describes, particularly, a separatrix chaotic layer [7].

Another form of nonlinearity

$$g(E)=2\pi\omega(-2E)^{-3/2} \tag{1.4b}$$

corresponds to the Coulomb interaction, and it is actually the Kepler law. Here it is convenient to use unperturbed energy $E<0$ as a dynamical variable, and ω is the perturbation frequency (see Ref. [4]).

The map (1.1) with nonlinearity (1.4b) and perturbation (1.2) is called the Kepler map, and it was applied in both celestial mechanics and atomic physics. In the former case the motion of comet Halley driven by Jupiter and Saturn was proved to be chaotic [8]. In atomic physics the Kepler map is a simple model to describe, in particular, a new type of photoelectric effect, the so-called diffusive ionization of Rydberg (highly excited) atoms [9].

The two latter examples show that map (1.1) can be considered also as a model for time-dependent dynamical systems that is for those driven by a periodic perturbation. This is, of course, simply a very convenient approximation in which the freedback from the perturbed freedom to perturbing one is completely neglected. Then, the model (1.1) can be described by the Hamiltonian

$$H(x, y, t) = G(y) + F(x)\,\delta_1(t) \to G(y) + K\sum_m \cos(x - 2\pi m t)\,, \qquad (1.5)$$

where $\delta_1(t)$ is δ-function of period 1 (one map's iteration), $G'(y) = g(y)$, $F'(x) = -f(x)$, and the last series represents perturbation (1.2).

A fairly simple map (1.1) can be simplified still further by linearizing the second equation. In this way we arrive, upon appropriate change of the action y, at the so-called standard map

$$\bar{y} = y + K\cdot\sin x\,; \qquad \bar{x} = x + \bar{y}\,, \qquad (1.6)$$

which describes the original model (1.1) locally in y, and which is also very popular now in studies of nonlinear phenomena in Hamiltonian systems. Model (1.6) is completely characterized by a single parameter K. In Hamiltonian representation (1.5) the «kinetic energy» for standary map is $G(y) = y^2/2$. Since x is an angle (phase) variable and y is the angular momentum, the model (1.6) is also called the «kicked rotator».

Each term in series (1.5) describes a particular first-order (primary) nonlinear resonance with the «pendulum» Hamiltonian (for standard map)

$$H_m = \frac{y^2}{2} + K\cdot\cos(x - 2\pi m t)\,. \qquad (1.7)$$

The resonant value of momentum $y_m = \dot{x}_m = 2\pi m$. In variables $\tilde{x} = x - 2\pi m t$ and $\tilde{y} = y - y_m$ any single resonance is a conservative system. Its motion is strictly bounded in y by the resonance width $\Delta y_m = 4\sqrt{K}$ owing to the nonlinearity that is the dependence of frequency $\dot{x} = y$ on momentum y.

1.2. Weak nonlinearity [10]. The structure of resonance drastically changes if we add to Hamiltonian (1.7) the term $\omega_0^2 x^2/2$:

$$H_m = \frac{y^2}{2} + \frac{\omega_0^2 x^2}{2} + K\cdot\cos(x - 2\pi m t), \qquad (1.8)$$

which breaks down the integrability of the system for any $\omega_0 \neq 0$.

Actually, the model (1.8) is quite different from model (1.7) as now variable x is no longer confined to interval $(0, 2\pi)$, and y is not the angular momentum. One may interpret Hamiltonian (1.8) as describing a particle-wave interaction. Such models have been studied by many authors in plasma physics (see, e. g., Ref. [5]), yet the true understanding has been achieved only recently (see, e. g., Ref. [10]). The peculiarity of model (1.8) is the weak nonlinearity that is the unperturbed ($K = 0$) oscillation is linear (isochronous) which turns out to be a much more difficult problem as compared with strong (unperturbed) nonlinearity (1.4). The resonance is now determined not by initial conditions but by the parameters of the model: $2\pi m = n\omega_0$ with any integer $n \neq 0$. In the action-angle variables (I, φ) of the harmonic oscillator a single resonance is approximately described by the Hamiltonian

$$H_m \approx K\cdot J_m(a)\cos\left(m\varphi + \frac{\pi m}{2}\right), \qquad (1.9)$$

where $a = (2I/\omega_0)^{1/2}$ is the oscillation amplitude, and J_m is the Bessel function. There are now infinitely many stable and unstable periodic orbits (instead of two for strong nonlinearity) while the separatrices, connecting unstable points, form an unbounded network on the phase plane (I, φ). As a result, even a single weakly nonlinear resonance can make the motion completely unstable and unbounded.

2. LEVELS OF DISORDER

In this Section I attempt to «organize» the great variety of chaos into a series of levels with increasing disorder and complexity.

2.0. Complete integrability [15]. This, zero, level of the maximal order is characterized by a stable and dynamically predictable motion in terms of individual trajectories. The motion is quasi-periodic that is of a purely discrete spectrum. One may call it simple dynamics. Yet, in the general theory of dynamical systems this «simple» motion includes the whole quantum chaos, typically on a finite time scale (see, e. g., Ref. [3]). The latter is dynamically equivalent to a many-dimensional linear oscillator which is apparently the simplest model of the quantum chaos [11]. On the other hand, in the formal thermodynamic limit of infinitely many freedoms this model provided the foundations of the traditional statistical mechanics, both clas-

sical and quantal, of macroscopic systems (for a rigorous theory see, e. g., Ref. [12]).

The standard map, as the simplest model, is completely integrable for $K=0$ only, that is in the unperturbed limit. In this case $y=\text{const}$ is the motion integral, and $x=2\pi rt$ where quantity

$$r=\frac{\omega}{2\pi}=\frac{\Delta x}{2\pi\,\Delta t} \tag{2.1}$$

is called rotation number. This very important parameter of a trajectory is the ratio of motion frequency (ω) to that of the perturbation (2π). Particularly, this ratio determines resonances (with zero perturbation in this limit!) which correspond to rational $r=p/q$. Any resonant trajectory is just q separate points on the phase plane (x, y). For irrational r the trajectory is a continuous straight line $y=2\pi r$ which is called invariant curve.

In spite of a great recent success in constructing the whole families of completely integrable systems (see, e. g., Ref. [13]) they all are exceptional, or nongeneric, in the sense that almost any perturbation destroys the integrability.

2.1. KAM integrability [14] is the generic property of a completely integrable system under sufficiently weak perturbation. The theory of such systems had been initiated by Kolmogorov and was essentially developed by Arnold and Moser (see, e. g., Ref. [15]), hence, abbreviation KAM.

For the standard map this first level of disorder corresponds to a nonzero $K\to 0$. Most invariant (KAM) curves survive weak perturbation that is they are only slightly deformed but remain continuous and, hence, unpenetrable for other trajectories. For this reason the KAM curve is called absolute barrier (for the motion). This property depends on the rotation number r of the curve which must be sufficiently irrational for the stability against perturbation. Hence, the importance of parameter r which is used as the label for identification of a given KAM curve at different perturbations.

Curves with resonant $r=p/q$ are all destroyed by any perturbation to form a different structure of the nonlinear resonance (Fig. 4). However, the nonintegrable part of this structure is confined to an exponentially narrow chaotic layer only. From physical point of view such a motion can be well considered in most cases as integrable to a very high accuracy. This is reminiscent of the

adiabatic invariance which is very important in physics even though it is not exact. Actually, there is a deep relation between the two, and we call KAM integrability the inverse adiabaticity [14, 16].

Approximately, the dynamics on this level is as simple as on the previous one. Yet, the chaotic component of motion, being of an exponentially small measure, is everywhere dense. As a result, the whole motion stucture becomes very comlicated. For more than two freedoms the phase space is cut through by a connected network of channels which support a global diffusion [7]. Even though the rate of this Arnold diffusion is also exponentially small it may be important in some special cases. For a weakly nonlinear system the Arnold diffusion is possible even in two freedoms as well, for instance, in model (1.8) [10].

2.2. Complete chaos [20]. Now we turn to the opposite limiting case when the motion is fully chaotic. In the standard map, as $K\to\infty$, there is a single chaotic component of motion stretched over the whole phase space (cylinder) of the model. The motion spectrum is purely continuous while a typical individual trajectory is most complicated. The latter means that Kolmogorov's complexity, which is equal to the information associated with trajectory, is finite, per unit time, and equal to the rate of local exponential instability of motion [1]. Hence, the dynamics on this level is most complicated to the extent that trajectory actually loses its physical meaning.

Nevertheless, the dynamical equations, e. g., map (1.6), can still be applied to copletely derive the statistical properties of the unstable motion. Moreover, on this level the statistics turns out to be very simple and already well-known from the traditional statistical mechanics. For example, in the standard map it is simply a homogeneous diffusion in y with the rate

$$D_y\equiv\frac{\langle(\Delta y)^2\rangle}{t}=\frac{K^2}{2}C(K)\to\frac{K^2}{2}, \tag{2.2}$$

where function $C(K)$ accounts for the dynamical correlation of phase x, and $C(K)\to 1$ as $K\to\infty$ [17]. For this reason the complexity of motion on this level is still not the highest one.

2.3. Critical phenomena: scale invariance [21]. For a typical (generic) perturbation, neither very weak nor very strong, the whole structure of motion is most complicated because the phase

space is generally divided in many separate domains with both regular and chaotic motions. In the standard map, for example, such an intricate behaviour corresponds to $K\sim1$ (see Fig. 1) that is around the global critical perturbation $K=K_G\approx1$. The latter is the border between strictly bounded motion for any initial conditions ($K\leqslant K_G$) and unbounded motion for some initial conditions ($K>K_G$).

In the unbounded chaotic component (for $K>K_G$) the motion is still diffusive with the rate [18]

$$D_y\approx0.3\,(K-K_G)^3 \qquad (2.3)$$

vanishing toward the critical perturbation (cf. Eq. (2.2)) where the correlation $C(K)\approx0.6(K-K_G)^3/K^2$). The main difficulty here is a hierarchical (fractal) structure of the chaotic component. The invariant measure—phase area, known beforehand, doesn't help in this case. The ultimate origin of that complexity is the chaos border in the phase space between chaotic and regular components of motion which also results in very peculiar statistical properties of the chaotic motion (see Section 4).

Thus, the chaos border makes both individual (chaotic) trajectories as well as the statistical properties of the motion very complicated. Is there any way to simplify the description of such a motion? Or: would it be possible to find any order in that mess? Surprisingly, it is possible, indeed, in some cases if one compares the critical structure at different scales in the phase plane (Section 3.3). Asymptotically, as you enlarge the structure more and more it exactly repeats itself with all the dynamical and statistical complexity (see also Fig. 5 below)! This peculiar property is called the scale invariance, and it is described by the so-called renormalization group, or in brief, renormgroup.

2.4. Critical phenomena: renormchaos [22]. The variation of the motion structure with the scale in phase space can be considered as a certain abstract dynamics (see Section 3.4) which we termed the renormalization dynamics, or renormdynamics [22]. Here the scale plays a role of «time» and we call it renormtime. The simplest case of any dynamics is a fixed point (for maps) which in renormdynamics corresponds to the scale invariance described above (see also Section 3.3). But typically the dynamics is chaotic, and so there must be a sort of renormalization chaos (renormchaos) as well. Guided by this analogy we have found such a chaos, indeed [22]!

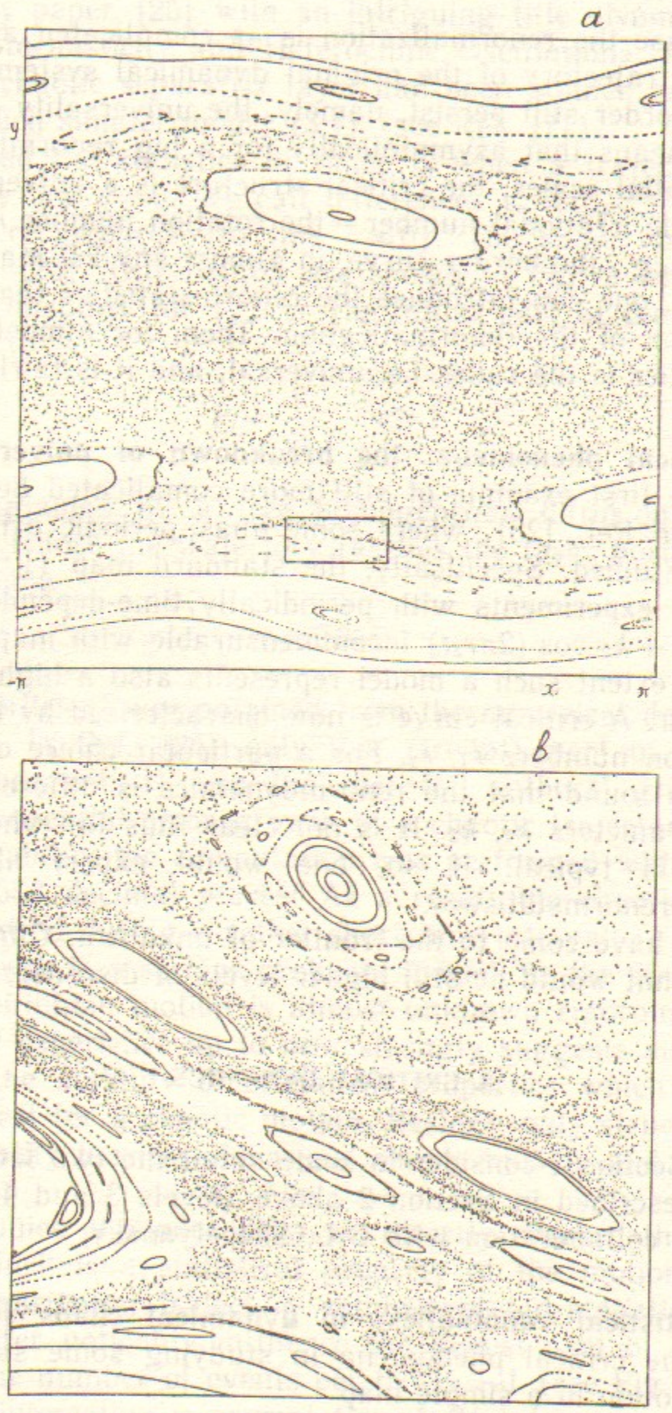

Fig. 1. An example of critical structure in map (3.1) with $\lambda=5$; scattered points belong to a single chaotic trajectory:

a—the whole chaotic layer; *b*—enlarged part near the chaos border $y\approx-\lambda$ where the motion is described locally by the standard map (1.6) with $K\approx1$ [19].

In this case the renormalization is as complicated as an individual chaotic trajectory of the original dynamical system. Yet, some remnants of order still persist, namely, the universality of renormalization. It means that asymptotically for a big renormtime, that is for small spatial scales, the critical structure is a universal functional of a single irrational number — the rotation number r_c of the critical curve, e. g., the border curve, in almost any $2D$ map [21].

Moreover, one can introduce the renormstatistics that is statistical description of the renormalization. Then, for almost any r_c the renormstatistics is the same, i.e. universal, and it is fairly simple.

2.5. Critical phenomena: the breakdown of universality [23]. Recently, the first example of still more complicated behaviour has been found in Ref. [23], where some quasi-periodic driving perturbation was studied. Specifically, the standard map (1.6) was used in numerical experiments with periodically time-dependent parameter $K(t)=k_1+k_2\cos(2\pi r_2 t)$ incommensurable with map time step.

To some extent such a model represents also a higher-dimensional behaviour. A critical curve is now characterized by the two irrational rotation numbers r_1, r_2. For a particular choice of irrationals r_1, r_2 it was found that the renormdynamics is different in dependence of parameters k_1, k_2. It is not clear thus far whether such a breakdown is typical. If so, one would expect also a more complicated renormstatistics.

Here we have come to the frontier of unknown. Currently, there is no idea what would be still higher levels of disorder, if any.

3. CRITICAL DYNAMICS

In this Section I consider in some detail the two levels of disorder brifly described in Section 2 above (levels 3 and 4). This work was done in collaboration with D.L. Shepelyansky.

3.1. Statistical «anomalies» in dynamical chaos [24]. We encountered the critical phenomena in studying some statistical properties of motion in a simple map

$$\bar{y}=y+\sin x\,; \quad \bar{x}=x+\lambda\cdot\ln|\bar{y}| \tag{3.1}$$

of the type described in Section 1.1 above. These our studies were

stimulated by paper [25] with an intriguing title «Numerical Experiments in Stochasticity and Heteroclinic Oscillation». Actually, the motion in a chaotic separatrix layer had been studied, and we went on with a much simpler model (3.1) (see Ref. [7]).

We studied the statistics of times t_n when a trajectory crosses the symmetry line $y=0$. We call differences $\tau_n=t_{n+1}-t_n$ the times of Poincaré recurrences (to line $y=0$). The same was implicitly done in Ref. [25]. Our results are shown in Fig. 2 where $P(\tau)$ is (integral) probability for $\tau_n>\tau$. The initial part of the distribution is very close to

$$P_f=\frac{1}{\sqrt{\tau}}; \quad \tau\geqslant 1 \tag{3.2}$$

and it is explained by a free homogeneous diffusion within the chaotic layer before the trajectory reaches the layer border ($y_b\approx\lambda$). It takes the time

$$\tau_f\approx 0.3\lambda^2, \tag{3.3}$$

where the coefficient was obtained from the numerical data.

Curiously, in Ref. [25] only this (trivial) part of distribution $P(\tau)$ was observed. It was the cost for authors' great concern about the exponential error growth at a chaotic trajectory. To overcame the instability the computation was performed with the record accuracy of 358 decimal places! As a result the chaotic trajectory could be followed during a rather short time interval.

Error growth is a serious problem, indeed, as the structural stability of Hamiltonian motion is almost unknown rigorously. Yet, all the numerical experience up to now strongly suggests such stability and, hence, the stability of statistical properties which are of the primary interest for a chaotic motion. Besides, only structural stability would justify the use of various simple models and approximations.

In our studies of model (3.1) we directly checked that distribution $P(\tau)$, which is a statistical property of the motion, does not depend on a particular trajectory within expected statistical fluctuations. The latter noticably influence the lowest part of distribution $P(\tau)$ where the number of events per bin is ~ 1 (see Fig. 2).

The most interesting is asymptotics of $P(\tau)$ for $\tau\gg\tau_f$ (3.3). This part characterizes the motion structure of chaos border at $|y|=y_b\approx\lambda$, or the critical structure as we call it.

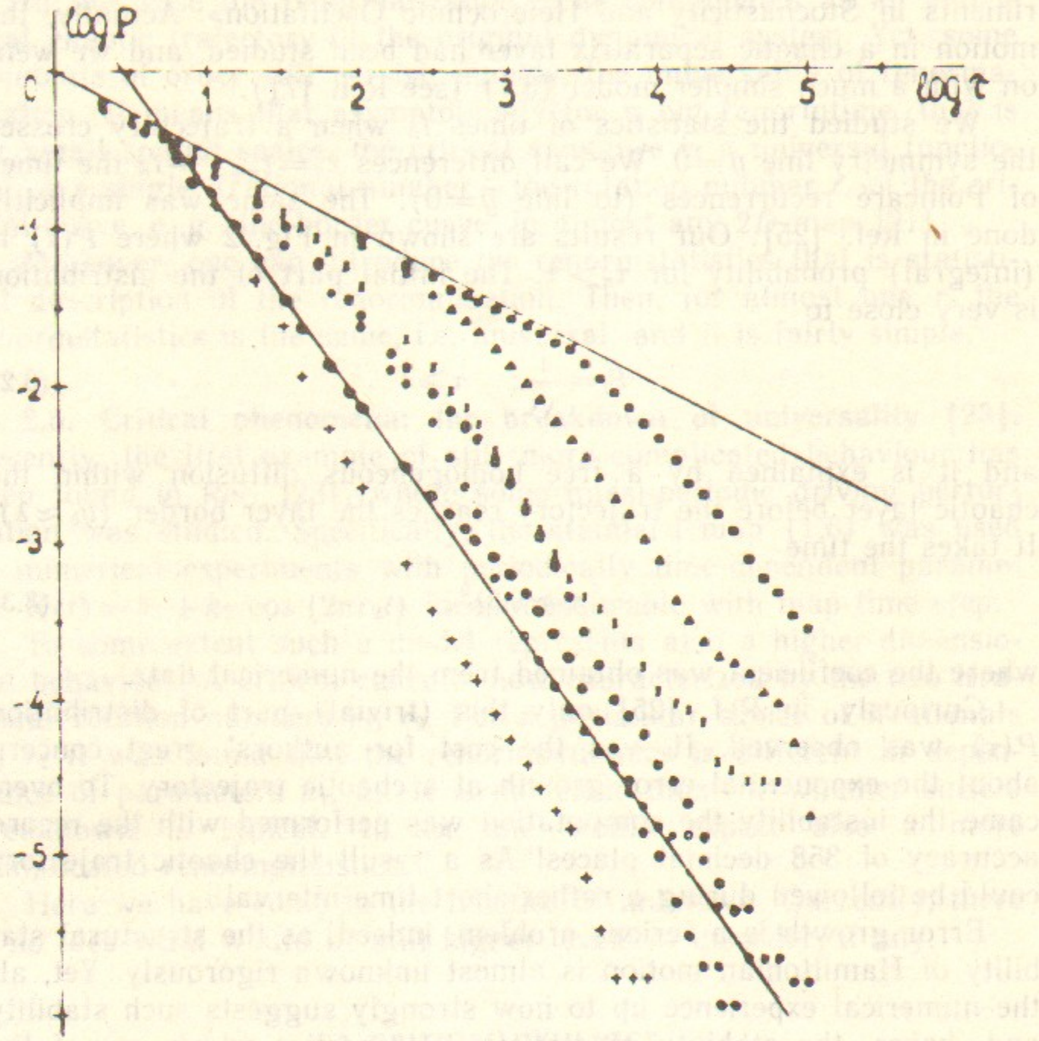

Fig. 2. Poincaré recurrences in the chaotic layer of map (3.1) for various $\lambda=1$ (lower points) through 100 (upper points). Two straight lines are power law with exponents -0.5 and -1.37, respectively (after Ref. [24]).

The following features of $P(\tau)$ asymptotics seem to be of importance. First, the distribution is a power law and not an exponential:

$$P(\tau) \approx \frac{\tau_f^{p-1/2}}{\tau^p}; \quad \tau \gtrsim \tau_f; \quad \langle p \rangle \approx 1.5 < 2. \tag{3.4}$$

This suggests a hierarchical (fractal) structure of the border. The accuracy of numerical value for p is not very good, yet we are sure that important inequality (3.4) always holds.

On the other hand, distribution $P(\tau)$ is a power law only approximately, at average. Irregular oscillations of the local exponent $p(\tau) \equiv d \ln P / d \ln \tau$ clearly show up in Fig. 2. These do not depend on trajectory and, hence, characterize not statistical fluctuations but, again, the structure of chaos border. Such a structure with variable exponent $p(\tau)$ is now called multifractality (see. e. g., Ref. [26]).

Statistics of Poincaré recurrences $P(\tau)$ proved to be the most convenient and reliable numerical data to study (cf. Ref. [25]). On the other hand, it is directly related to the most important statistical property of motion — the time correlation [27], e. g., such one

$$C_y(\tau) = \frac{\overline{y(t)\, y(t+\tau)}}{\overline{y^2(t)}}, \tag{3.5}$$

which characterizes the «sticking» of trajectory near the border. Notice that $\overline{y(t)} = 0$ for map (3.1).

Indeed, the correlation is proportional to the sticking time that is (cf. Ref. [27])

$$C_y \sim \frac{\tau P(\tau)}{\langle \tau \rangle} \sim \tau^{-p_c}; \quad p_c = p - 1 < 1 \tag{3.6}$$

for $\tau \gtrsim \tau_f$. Here $\langle \tau \rangle \approx 3\lambda$ is mean recurrence time, and the latter important inequality follows from Eq. (3.4) (see also Fig. 3,*b*). For chaotic motion $C_y \to 0$ as $\tau \to \infty$ (mixing property), hence, $p_c > 0$, and, for bounded motion, $p > 1$. Also, notice that due to ergodicity of motion $C_y \sim \mu(\tau)$, the measure of the sticking domain (a strip) which is $\sim |y - y_b| / y_b$.

Slow correlation decay due to the sticking of a chaotic trajectory near the chaos border, and especially the inequality (3.6) are responcible for all other statistical «anomalies» of the motion with a chaos border to be discussed below. A power law decay (3.6) is

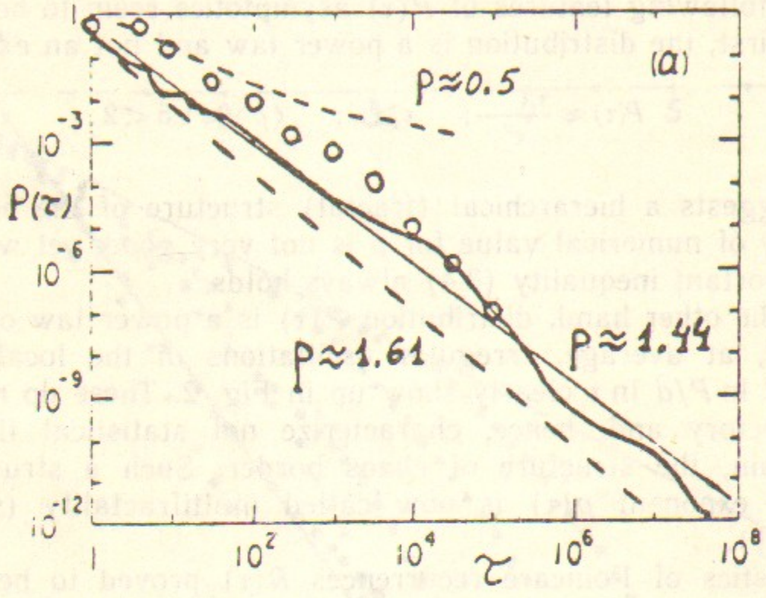

Fig. 3. Statistical properties of motion with chaos border:

a—Poincaré recurrences; *b*—correlation decay. Solid curves are for map (3.7) [27] while circles are our data for $\lambda=3$. Straight lines indicate power law with the exponent shown. Dashed curve is the effect of noise [22].

especially remarkable in view of the strong exponential instability of the motion which is characterized by positive Lyapunov's exponent Λ_+ and the KS-entropy (per map iteration): $h=\Lambda_+\approx 0.7$ (see Section 6.3 in Ref. [7]). The apparent contradiction is explained as follows. The instability rate h is mainly determined by the central part of the chaotic layer while the sticking is a peripheral effect which has a negligible impact on the mean local instability. In other words, KS-entropy does not discern such statistical anomalies. It can be done using the so-called Renyi entropy K_q which is a generalization of $h=K_1$ (see, e. g., Ref. [28]), and which drops to zero for all values of parameter $q>1$ in the presence of chaos border [29].

The critical phenomena at the chaos border and related statistical anomalies are «universal» (a very popular word in this field of research!) in that they are approximately the same in any $2D$ map. In Fig. 3,*a*, for example, our results are compared with those in Ref. [27] for a different map on torus

$$\bar{y}=y+2(x^2-a^2)\,; \qquad \bar{x}=x+\bar{y} \tag{3.7}$$

with a closed chaos border surrounding the domain of regular motion around the stable fixed point at $y=0$; $x=-a$ $(0<a<1)$. Notice that the two distributions $P(\tau)$ are not identical but rather similar (see below).

3.2. The resonant theory [30]. To understand the statistical anomalies described above we have developed a resonant theory of critical phenomena in dynamics [30, 31]. Let us begin with a simpler problem of isolated critical KAM curve whose rotation number is some irrational r. According to the KAM theory most invariant curves are preserved under a sufficiently weak perturbation in the sense that they remain continuous and are only slightly deformed by the perturbation. The theory of critical phenomena follows the transformation of a KAM curve up to the critical perturbation which destroys the curve.

The critical perturbation, e. g., $K_c(r)$ for the standard map, crucially depends on the arithmetic of r. Remember that for the everywhere dense set of rationals $r=p/q$ the critical $K_c(p/q)=0$ (Section 2.1). The whole dependence $K_c(r)$ is a fractal function [32].

The physical explanation of this behaviour is in resonances. Their profound impact on the critical structure is clearly seen in all numerical data (see, e. g., Fig. 1). For irrational r the principal

resonances correspond to the best rational approximations of r which are known to be the so-called convergents $r_n = p_n/q_n$ of the infinite continued fraction

$$r = \cfrac{1}{m_1 + \cfrac{1}{m_2 + \ldots}} \equiv (m_1, m_2, \ldots) ;$$

$$r_n = (m_1, \ldots, m_n) \to r , \qquad n \to \infty . \tag{3.8}$$

The arithmetic of continued fractions gives for almost any r

$$|\rho_n| \equiv |r_n - r| \sim \frac{1}{q_n^2} \sim |r_{n+1} - r_n| . \tag{3.9}$$

From physical viewpoint ρ_n is the detuning of the n-th principal resonance with respect to the critical motion. Then, from the resonance overlap criterion [7] the main critical scaling, or the criticality condition, is

$$\Delta\rho_n \sim |\rho_n| \sim \frac{1}{q_n^2} , \tag{3.10}$$

where $\Delta\rho_n$ is the resonance width. These resonances determine the principal scales of the critical structure whose scheme is outlined in Fig. 4 (cf. Fig. 5 below).

To estimate $\Delta\rho_n$ we need the critical Hamiltonian which describes all resonances $r_{pq} = p/q$ (p, q are any integers), and not the primary ones $r_m = m$ only from the original Hamiltonian of the type (1.5). Integer resonances $r_m = m$ are obtained in the first approximation $x_c(t) \approx 2\pi r_c t \equiv \xi_c$, the mean motion on the critical KAM curve.

Extrapolating the KAM theory (see, e. g., Ref. [15]) the following expression can be assumed for the critical motion:

$$x_c(t) = \xi_c + \sum_q a_q \sin(q\xi_c) . \tag{3.11}$$

Locally in y, in the standard—map approximation the critical Hamiltonian H_c, which describes some vicinity of the critical KAM curve $r = r_c$, can be written as a natural generalization of the original Hamiltonian (1.5) (with $G(y) = y^2/2$) in the following form

$$H_c(\theta, \rho, t) = \frac{\rho^2}{2} + \sum_{p,q} \frac{v_{pq}}{(2\pi)^2} \cos 2\pi(q\theta - \nu_{pq} t) . \tag{3.12}$$

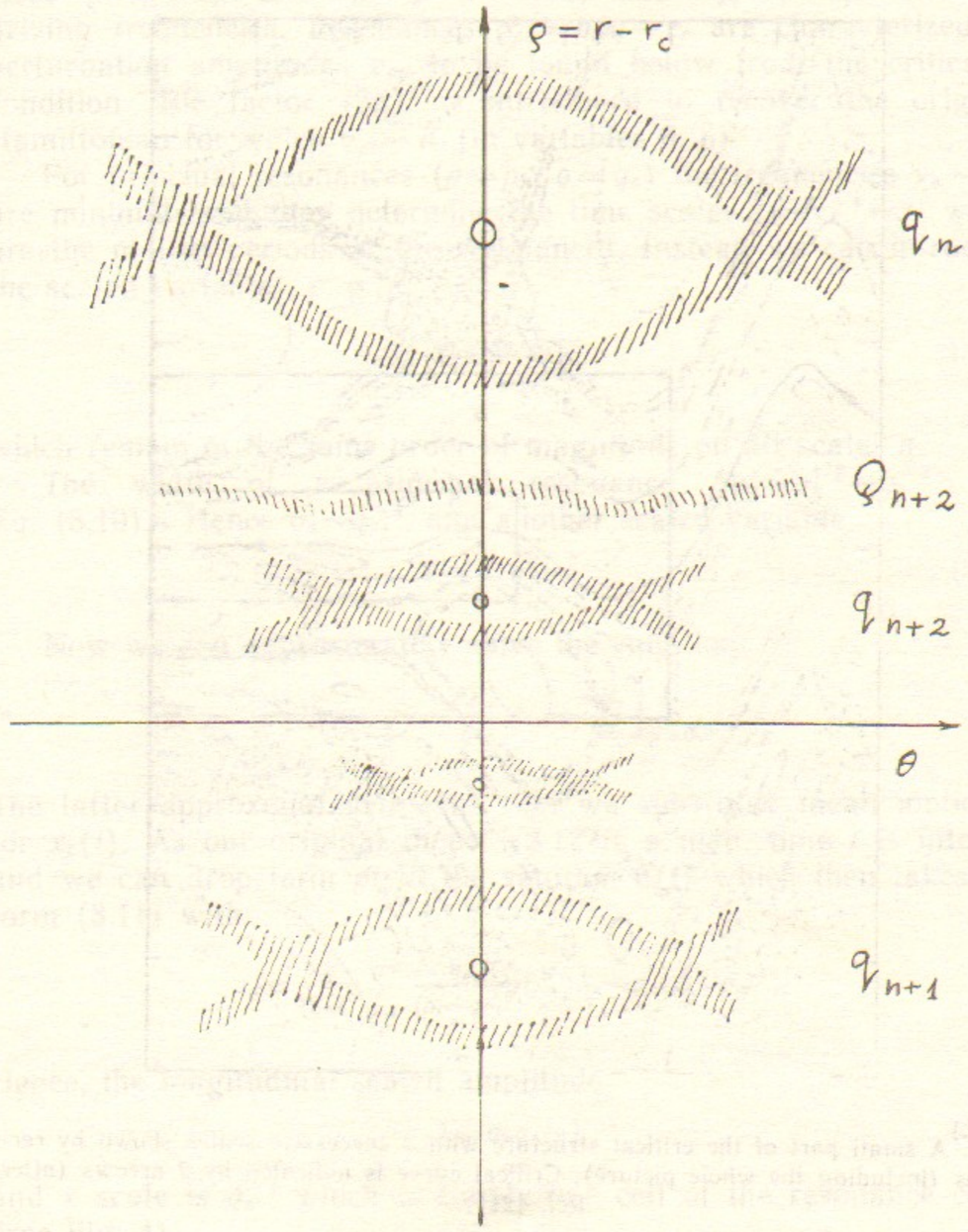

Fig. 4. Outline of the critical structure with a few principal resonances, represented by the separatrix chaotic layers (hatched) and stable periodic orbits (circles), and the corresponding scales q_n. Another chaotic layer Q_n is a bottleneck between the scales (Section 4.3).

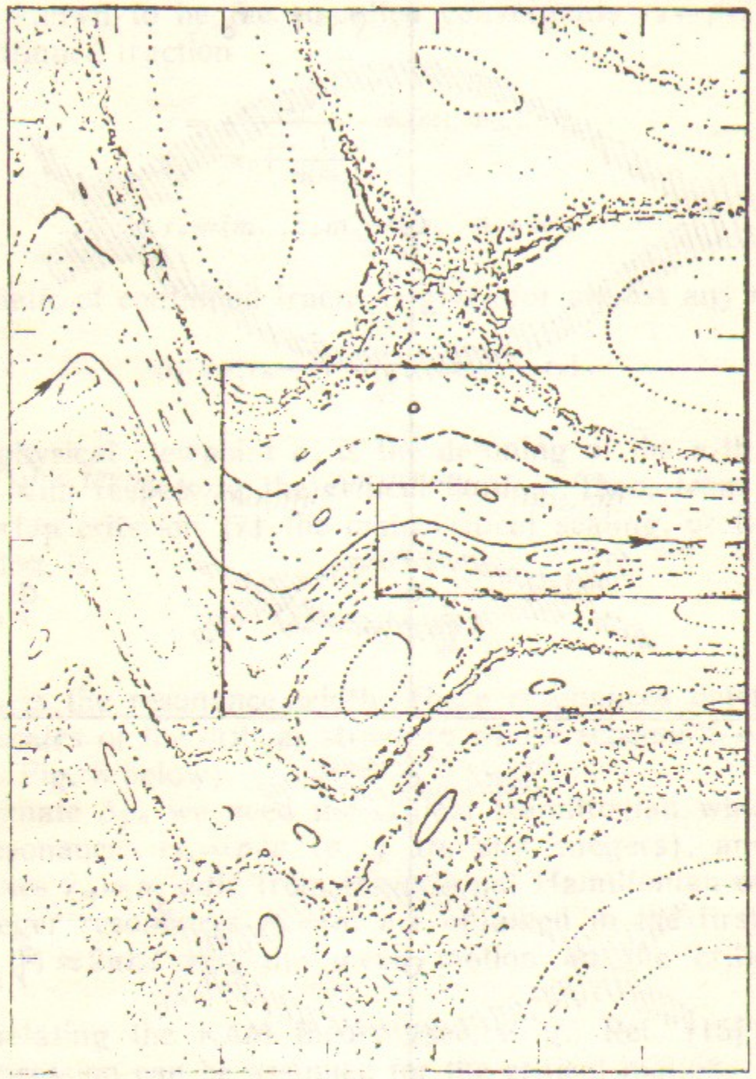

Fig. 5. A small part of the critical structure with 3 successive scales shown by rectangles (including the whole picture). Critical curve is indicated by 2 arrows (after Ref. [21]).

Here $\rho = r - r_c$; $2\pi\theta = x - \xi = x - 2\pi r t$, and $\nu_{pq} = p - q r_c$ are the driving frequencies. Resonances $\rho_{pq} = p/q - r_c$ are characterized by perturbation amplitudes v_{pq} to be found below from the criticality condition. The factor $(2\pi)^2$ is introduced to recover the original Hamiltonian for which $v_{p1} = K$ (in variables θ, ρ).

For principal resonances ($p = p_n$, $q = q_n$) the frequencies $\nu_n \sim q_n^{-1}$ are minimal, and they determine the time scales $t_n \sim \nu_n^{-1} \sim q_n$ which are the motion periods at the resonances. Instead we can introduce the scaled variables, e. g.,

$$T = \frac{t_n}{q_n} \sim 1 , \tag{3.13}$$

which remain of the same order of magnitude on all scales n.

The width of a principal resonance $\Delta\rho_n \sim v_n^{1/2} \sim q_n^{-2}$ (see Eq. (3.10)). Hence $v_n \sim q_n^{-4}$, and another scaled variable

$$V = v_n q_n^4 \sim 1 . \tag{3.14}$$

Now we can approximately solve the equation

$$\ddot{\theta} = \dot{\rho} = -\frac{\partial H_c}{\partial \theta} \approx -\frac{\partial H_c}{\partial \theta}\Big|_{\theta=0} .$$

The latter approximation means that we substitute mean motion ξ for $x_c(t)$. As our original model (3.1) is a map, time t is integer, and we can drop term pt in the solution $\theta(t)$ which then takes the form (3.11) with

$$a_q \approx \frac{q}{(2\pi)^3} \sum_p \frac{v_{pq}}{(p - qr)^2} ; \quad a_n \sim v_n q_n^3 \sim q_n^{-1} .$$

Hence, the longitudinal scaled amplitude

$$A = a_n q_n \sim 1 \tag{3.15}$$

and x scale is q_n^{-1} which is simply one cell of the resonance chain (see Fig. 4).

In the standard-map approximation

$$y_c(t) \approx \dot{x}_c(t) = 2\pi r_c + \sum_q b_q \cos(q\xi_c - 2\pi p t) ,$$

with $b_n = 2\pi a_n \nu_n$, and the transverse scaled amplitude

$$B = b_n q_n^2 \sim 1 . \tag{3.16}$$

Hence, y scale is q_n^{-2} which is the resonance width.

Consider now the periodic orbit at resonance center (Fig. 4). Its stability is determined by the so-called Creene residue [33] (see also Ref. [5])

$$R = \sin^2\left(\frac{t_n \omega_n}{2}\right) \sim 1 , \tag{3.17}$$

where $t_n = q_n$ in the period, and $\omega_n \approx q_n v_n^{1/2}$ is the small oscillation frequency (see Eq. (3.12)). Obviously, R is a scaled variable.

Finally, the scaled rotation number, or rather the scaled detuning

$$D = \rho_n q_n^2 \sim 1 \tag{3.18}$$

determines actually all the other scaled variables.

So far we considered exactly critical conditions that is $K = K_c(r)$. What would be impact of any deviation $\Delta K = K - K_c(r) \neq 0$? It can be evaluated as follows. Perturbation amplitudes v_n in Eq. (3.12) appear in q_n-th order of the perturbation theory and are proportional to $(K/K_c)^q = \exp\left(q \ln \frac{K}{K_c}\right)$. Hence, for a small deviation from criticality ($\Delta K \to 0$) the amplitude $v_n \sim \exp(C q_n \Delta K)$ with some $C \sim 1$. At $\Delta K = 0$ the exponential dependence cancels, and only a power low (3.14) remains. Generally,

$$v_n \sim \frac{1}{q_n^4} \exp(C q_n \Delta K) . \tag{3.19}$$

For $\Delta K > 0$ all scales $q_n \gtrsim (\Delta K)^{-1}$ are destroyed and a chaotic layer of width $\Delta y \sim (\Delta K)^2$ is formed. From Eq. (3.19) the scaled perturbation can be introduced

$$P = q_n \Delta K_n \sim 1 , \tag{3.20}$$

which describes approaching the renormalization limit for a fixed V, for example.

If the original perturbation is nonanalytic that is with some power law spectrum $v_q^0 \sim q^{-\beta-1}$ (cf. model (1.3) where $f_m \sim m v_m^0$) the critical conditions are only possible for $\beta > 3$, otherwise $K_c = 0$. Thus, $\beta_c = 3$ is the critical smoothness of the perturbation. I shall come back to this point in Section 4.1 below.

3.3. The renormalization group [21]. This powerful method, well known and widely applied in hydrodynamical turbulence, phase transitions and quantum field theory, was first used in nonlinear dynamics and chaos theory in Ref. [33]. Later on, the exact renormalization equations were formulated and studied in Ref. [34] for (dissipative) $1D$ maps, and in Ref. [21] for $2D$ area-preserving (Hamiltonian) maps. The renormgroup equations are an abstract map acting in the space of dynamical maps, and it is based on the arithmetical map for successive convergents $r_n = p_n/q_n$ of the critical rotation number $r_c = (m_n)$:

$$\bar{p} = \bar{m} p + \underline{p} ; \quad \bar{q} = \bar{m} q + \underline{q} , \tag{3.21}$$

where $\bar{p} \equiv p_{n+1}$; $p \equiv p_n$; $\underline{p} \equiv p_{n-1}$ etc. Besides qualitative understanding of critical phenomena (particularly, their universality) this approach provides very efficient numerical algorithms for computing all the parameters of critical structure. Unlike this, our resonant theory, being inherently approximate, allows some analytical estimates.

The resonance overlap criterion, on which the theory is essentially based, can directly provide order-of-magnitude estimates only as, for example, for scaled variables (3.14—3.17). However, there exists another group of critical parameters which can be evaluated to a surprising accuracy. Those are the scaling factors that is the ratios of particular quantities on the neighbouring scales. For example,

$$s_a = \frac{a_n}{a_{n+1}} ; \quad s_b = \frac{b_n}{b_{n+1}} ; \quad s_K = \frac{\Delta K_n}{\Delta K_{n+1}}$$

are the renormalization factors for x, y, and perturbation K, respectively.

The structure of scaled variables shows that all scaling factors are some powers of the main arithmetical factor

$$s_q = \frac{q_n}{q_{n-1}} . \tag{3.22}$$

To compare both approaches let us consider the simplest case of a homogenious continued fraction $r = (m, m, \ldots, m, \ldots) \equiv (m^\infty)$. In this case all the scaled variables become asymptotically, as $n \to \infty$, exact invariants of the renormgroup. This is called the scale inva-

riance. For example, $D \to (4+m^2)^{-1/2}$ (see Eq. (3.21)) which is a simple arithmetical property. The other invariants are not yet known except the case of $r=r_G=(1^\infty)=(\sqrt{5}-1)/2=0.618...$ which is called the golden tail (because for asymptotic properties only tail of the continued fraction matters).

In this particular case, studied in great detail, the normalization invariants are: $T=1$ (if, by definition, $t_n=q_n$, see Eq. (3.13)); $R=0.2500888...$; $V\approx(2\arcsin\sqrt{R})^2=1.097052...$; $A\approx 0.167$; $B\approx \approx 2\pi A/\sqrt{5}\approx 0.470$. Notice that from the above relation $R\sim V\sim \sim\Delta\rho_n/\rho_n$ the Greene residue also characterizes the resonance overlap.

Now consider the scaling factor for the area $c_n\sim a_n b_n$ of a resonance cell (the corresponding scaled variable $C=c_n q_n^3\approx \approx AB\approx 0.0787$):

$$s_c=c_n/c_{n+1}=s_q^3=4.236... \qquad (3.23)$$

while the exact numerical value via the renormgroup is 4.339... The two numbers are not equal but very close which was a puzzle for the formal renormgroup approach.

A similar situation is for the perturbation factor: $s_K=s_q=1.618...$ (resonant theory), and $s_K=1.627...$ (numerically).

The differences in scaling factors of the two theories can be interpreted as small changes of the exponents of q in scaled variables. For the two above examples we can write:

$$C=c_n q_n^\alpha; \quad \alpha=3.049960...$$
$$P=\Delta K_n q_n^\beta; \quad \beta=1.0126966... \qquad (3.24)$$

Other examples will be given below.

The behaviour of asymptotic renormalization invariants A and R is shown in Fig. 6 below. Remarkably, the invariant critical structure, which repeats itself on finer and finer scales with rapidly increasing precision, is itself of the highest complexity as it contains both chaotic trajectories and intricate admixture of regular and chaotic components of motion. An example of a tiny part ($\sim 0.01\times 0.01$) of that structure is shown in Fig. 5 [21]. The scale invariance is clearly seen within 3 successively scaled areas indicated by rectangles.

Notice that the scale invariance holds on a particular discrete set of scales, infinite though, because the renormgroup equations are based on the arithmetical map (3.21).

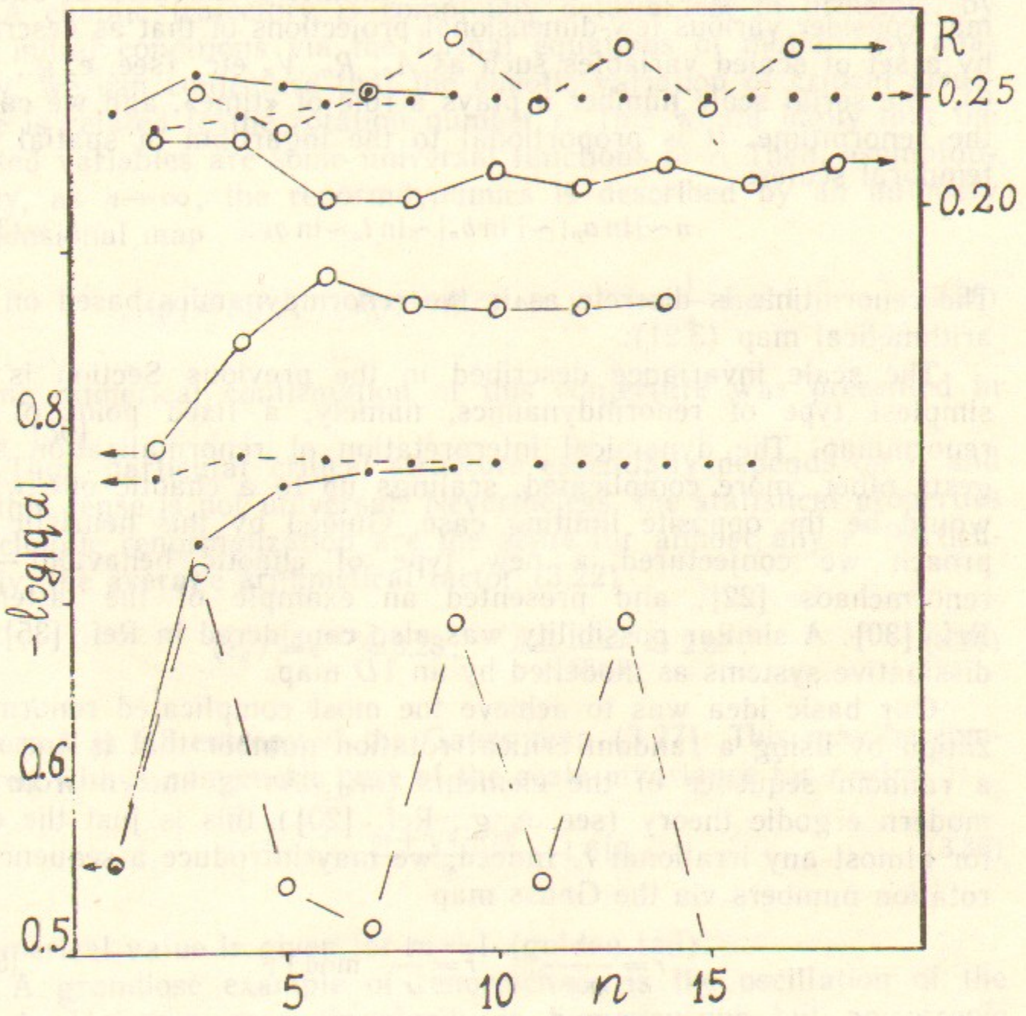

Fig. 6. An example of renormchaos for a random r_c (circles). Arrows indicate the corresponding scales for $A=aq$ (lower part), and for R (upper part); n is renormtime (the number of a principal scale). For comparison the same data are given for $r_c=r_G$ (dots) which illustrate the scale invariance (after Ref. [30]).

3.4. Renormalization chaos [22]. Variation of the critical structure from scale to scale can be viewed as some abstract dynamics. The corresponding dynamical space is infinitely dimensional but we may consider various few-dimensional projections of that as described by a set of scaled variables such as A_n, R_n, V_n etc. (see, e. g., Fig. 6). The serial scale number n plays a role of «time», and we call it the renormtime. It is proportional to the logarithm of spatial and temporal scales:

$$n \sim |\ln a_n| \sim |\ln b_n| \sim \ln t_n \sim \ln q_n \,. \tag{3.25}$$

The renormtime is discrete as is the renormdynamics based on the arithmetical map (3.21).

The scale invariance described in the previous Section is the simplest type of renormdynamics, namely, a fixed point of the renormmap. The dynamical interpretation of renormalization suggests other, more complicated, scalings up to a chaotic one which would be the opposite limiting case. Guided by this heuristic approach we conjectured a new type of chaotic behaviour — the renormchaos [22], and presented an example of the latter in Ref. [30]. A similar possibility was also considered in Ref. [35] for dissipative systems as modelled by an $1D$ map.

Our basic idea was to achieve the most complicated renormalization by using a random critical rotation number that is one with a random sequence of the elements $\{m_n\}$. As is known from the modern ergodic theory (see, e. g., Ref. [20]) this is just the case for almost any irrational r. Indeed, we may introduce a sequence of rotation numbers via the Gauss map

$$r = \frac{1}{m + \bar{r}}; \qquad \bar{r} = \frac{1}{r} \mod 1 \,, \tag{3.26}$$

which is known to be chaotic [20]. Moreover, the basic arithmetical factor in renormalization (3.22) also obeys the same map

$$w = \frac{1}{\bar{w}} \mod 1; \qquad w = \frac{1}{s_q} < 1 \tag{3.27}$$

backwards in renormtime, and with the «initial» $w_\infty = \tilde{r}$ where $\tilde{r}$ is the irrational with reversed sequence of elements in respect to r. Clearly, the variation of critical structure in this case would be as random and unpredictable as a chaotic trajectory. An example of renormchaos is presented in Fig. 6 as described by A and R scaled

variables. Irregular character of this renormdynamics is clear from Fig. 6 but the proof of its randomness is related to Gauss map (3.27).

A chaotic trajectory is completely determined, in principle, by the initial conditions via the formal equations of motion. By analogy, we can conjecture that the chaotic variation of critical structure is related to the rotation number r. This would imply that the scaled variables are some universal functions of r. Then, asymptotically, as $n \to \infty$, the renormdynamics is described by an infinitely dimensional map

$$\bar{A}(r) = A(\bar{r}); \qquad \bar{R}(r) = R(\bar{r}) \text{ etc.}; \qquad \bar{r} = \frac{1}{r} \mod 1 \,. \tag{3.28}$$

Some numerical confirmation of this conjecture was presented in Ref. [30].

Thus, particular critical structure essentially depends on r, and in this sense is not universal. Nevertheless, the statistical properties of chaotic renormalization are the same for almost any r. Particularly, the average arithmetical factor (3.22)

$$\langle s_q \rangle = e^{h/2} \approx 3.28; \qquad h = \frac{\pi^2}{6 \ln 2} \approx 2.37 \,, \tag{3.29}$$

where h is KS-entropy of the Gauss map (3.27). This may be compared with a nongeneric case of the scale invariance for $r = (m^\infty)$:

$$s_q = \frac{m + \sqrt{4 + m^2}}{2} \to 1.618... \tag{3.30}$$

Numerical value is given for $m = 1$ (golden tail).

A grandiose example of renormchaos is the oscillation of the whole Universe near singularity in homogeneous but anisotropic cosmological models [36]. So far there is no sign of such oscillations in our early Universe. Yet, the equations of the general relativity allow that type of solution. Remarkably, the very complicated relativistic equations are approximately reduced to the trivial Gauss map.

3.5. Higher dimensions. A general picture of overlapping resonances, which destroy KAM tori, holds for arbitrary number of freedoms [7]. This allows to extend our resonant theory of critical phe-

nomena to higher dimensions. There are two generally different cases of the latter: (i) $N>2$ freedoms, and (ii) a driving quasi-periodic perturbation of one freedom. In the resonant theory both are similar, the principal parameter being the number of frequencies N [37].

First of all, for arbitrary N the number of all resonances with $\sim q$ harmonics of each basic frequency is $\sim q^N$, hence the detuning $\rho \sim q^{-N}$ (cf. Eq. (3.9)), and

$$D = \rho q^N \sim 1 . \tag{3.31}$$

Now the main rotation number r is defined with respect to one of perturbation frequencies. Remaining $N-2$ rotation numbers enter driving frequencies $v_q \sim q\rho \sim q^{1-N}$ in the critical Hamiltonian (3.12). The resonance width $\Delta\rho \sim v_q^{1/2}$, and from the overlap criterion (3.10) the criticality condition is $v_q \sim q^{-2N}$, or (cf. Eq. (3.14))

$$R \sim V = v_q q^{2N} \sim 1 . \tag{3.32}$$

Hence, the critical perturbation smoothness $\beta_c = 2N-1$ increases with N (cf. Ref. [37]).

Longitudinal amplitudes $a_q \sim q v_q / v_q^2 \sim q^{-1}$ of the critical motion $x_c(t)$ do not depend on N, and

$$A = q a_q \sim 1 \tag{3.33}$$

as before. The transverse amplitudes $b_q \sim a_q v_q \sim q^{-N} \sim \Delta\rho$ decrease with N but remain of the order of resonance width. Finally, the perturbation scaling does not, aproximately, depend on N also:

$$P = q\Delta K_q \sim 1 . \tag{3.34}$$

However, in many-dimensional case ($N>2$) there is no simple procedure to single out the principal resonances like for $N=2$.

The renormalization group in higher dimensions was generally discussed already for dissipative systems (see, e. q., Ref. [35]). Yet, I am not aware of any particular results concerning the scaling properties in such systems.

To the best of my knowledge the only numerical data for $N=3$ (standard map with a time-periodic parameter $K(t)$) were presented recently in Ref. [23]. They seem to confirm the scalings related to R, P and A.

On the other hand, the authors did not find the scale invariance

in this model, and it seems do not exist at all. What is even more important, they discovered a breakdown of the renormalization universality in the sense that irregular oscillations of the critical structure depend, generally, not only on the two rotation numbers but also on model's parameters. Thus, many-dimensional renormdynamics appears to be even more complicated (chaotic?) as compared to the simplest case $N=2$.

4. GRITICAL STATISTICS

The most difficult, and as yet unsolved, problem is the impact of the critical structure at chaos border on the statistical properties of motion.

4.1. Smooth perturbation: $\beta<\beta_c$. To begin with let us consider a simpler problem of a smooth perturbation (1.3) with $\beta<\beta_c=3$. First, we can evaluate β_c directly from the resonance overlap criterion as applied to the original perturbation (1.3). The simplest estimate is as follows. The total width of all primary resonances $r_{pq}=p/q$ on the unit r interval is

$$\sim \sum_q q v_q^{1/2} \sim K^{1/2} \sum_q q^{(1-\beta)/2} \sim 1 . \tag{4.1}$$

This sum diverges for $\beta \leqslant 3$, hence $\beta_c=3$ in agreement with the previous estimate in Section 3.2. The latter estimate in Eq. (4.1) determines those resonances which provide the overlapping for $\beta<3$. The critical $q_c \sim K^{(\beta-3)^{-1}}$. The corresponding resonance width $\Delta\rho_c \sim K^{1/2} q_c^{-(\beta+1)/2}$, and the frequency (cf. Eq. (3.17)) $\omega_c \sim q_c \Delta\rho_c$. Hence, the diffusion rate in r (or in y) is

$$D \sim \omega_c (\Delta\rho_c)^2 \sim K^{3/2} q_c^{-\frac{1+3\beta}{2}} \sim K^{\frac{5}{3-\beta}} . \tag{4.2}$$

The border case $\beta=3$ requires more accurate estimates.

Estimate (4.2) agrees with numerical results in Ref. [38] for $\beta=1$ (discontinuous $f(x)$).

4.2. Critical perturbation [31]. One peculiarity of the standard map (1.6) is the periodicity not only in x but also in y with the same period 2π. As a result there is exact critical perturbation

$K=K_G\approx 1$ [33], such that for $K>K_G$ the motion is unbouded in y and diffusive for some initial conditions (Section 2.3). The problem I am going to discuss now is to explain scaling (2.3) for the diffusion rate as $K\to K_G$.

For $K>K_G$ the last (most robust) KAM curve is destroyed and transformed into a chaotic layer comprising all critical scales $q_n\gtrsim q_\varepsilon$ where $q_\varepsilon\sim\varepsilon^{-1}$, and $\varepsilon=K-K_G\to 0$ (see Eq. (3.19) and around). This chaotic layer is just the critical «bottleneck» which controls the transition time between integer resonances $r=m$, and, hence, the global diffusion. The time scale in the layer is $\sim q_\varepsilon$, and the same is for the exit time (t_-) from the layer. However, the entering into this thin layer ($\Delta r_\varepsilon\sim q_\varepsilon^{-2}$, Eq. (3.16)) from a big region ($\Delta r\sim 1$) takes much more time:

$$t_+\sim t_-\frac{\Delta r}{\Delta r_\varepsilon}\sim q_\varepsilon^3\sim\varepsilon^{-3}\sim D^{-1}. \tag{4.3}$$

This determines the transition time which is inversely proportional to the diffusion rate D in agreement with recent numerical results (see Eq. (2.3) and Ref. [18]). Notice that the first value for the exponent ≈ 2.6 [7] was not very accurate. The above estimate $\Delta r_\varepsilon/t_-\sim\Delta r/t_+$ (4.3) is simply the flux balance in statistical equilibrium.

It is interesting to mention that the renormgroup theory [39] gives the value $\ln s_c/\ln s_K=3.011...$ This is another example of surprising accuracy in the apparently primitive resonant theory.

4.3. The chaos border [30]. The impact of the critical structure at chaos border in phase space on the statistical properties of the chaotic motion is the most difficult, and as yet unsolved, problem. The straightforward approach would be as follows. The transition time τ_n between adjacent scales is proportional to the time scale $t_n\sim q_n$ which, in turn, scales like $\mu_n^{-1/2}\sim C_y^{-1/2}$ where $\mu_n\sim\rho_n\sim q_n^{-2}$ is the sticking measure, and where C_y is the correlation (Sections 3.1 and 3.2). Hence, $C_y\sim\tau^{-2}$, and $p_c=2$; $p=3$. In a more sophisticated way the same result was obtained in Ref. [40]. But this is a sheer contradiction with numerical data: $p\approx 1.5<2$.

The only way I see to avoid this contradiction is the conjecture that at exact criticality all transition times $\tau_n=\infty$ that is all scales are dynamically disconnected. Then, why a connected chaotic component near the chaos border exists? The natural answer is in that

the exact criticality is achieved on the border only while inside a chaotic region the motion is supercritical. Consider, for example, model (3.1). Locally it is described by the standard map with $K\approx\lambda/y$. In a small vicinity of the border $y=y_b\approx\lambda$ the perturbation K increases, indeed, like $\Delta K\sim\Delta y\sim\rho\sim q^{-2}$. However, this is not enough to destroy the corresponding scale q_n as $q_n\Delta K_n\sim q_n^{-1}\ll 1$ (see Eq. (3.19)). Only resonances with $q\gtrsim Q_n\sim q_n^2$ would be destroyed and form a very narrow ($\sim Q_n^{-2}\sim q_n^{-4}$) chaotic layer which could play a role of the bottleneck controlling transition time τ_n. Similarly to derivation of Eq. (4.3), we obtain

$$\tau_n\sim Q_n\frac{Q_n^2}{q_n^2}\sim q_n^4\sim\mu_n^{-2}\sim C_y^{-2}. \tag{4.4}$$

Hence

$$C_y(\tau)\sim\tau^{-1/2};\qquad P(\tau)\sim\tau^{-3/2}, \tag{4.5}$$

now in agreement with numerical data.

The same result can be obtained in a different, more formal, way. Namely, we can rescale dependence (4.3) for transition between integer resonances ($q_n=1$) to arbitrary scale q_n. To this end we rewrite Eq. (4.3) in scaled variables

$$\frac{\tau_n}{t_n}\sim(q_n\Delta K)^{-3}. \tag{4.6}$$

With $t_n\sim q_n$ and $\Delta K\sim q_n^{-2}$ we arrive at Eq. (4.4). Notice that a different relation $\tau_n(q_n)$ in Ref. [22] was due to a mistake in scaling.

A weak point of the latter approach (4.6) is in that the scaling (4.3) is asymptotic ($q_n\to\infty$) while integer resonances ($q_n=1$) are not. In any event, further studies into the mechanism of critical statistics are certainly required.

In higher dimensions (Section 3.5) the supercriticality $\Delta K\sim\rho\sim q^{-N}$; the bottleneck harmonic $Q\sim(\Delta K)^{-1}\sim q^N$, and transition time (cf. Eq. (4.4))

$$\tau\sim Q^{N-1}\frac{Q^N}{q^N}\sim Q^{2N-2}\sim\mu^{2-2N}. \tag{4.7}$$

Hence

$$C_y\sim\mu\sim\tau^{-\frac{1}{2N-2}};\qquad p_c=\frac{1}{2N-2}. \tag{4.8}$$

As $N\to\infty$, $p_c\to 0$, and correlations do not decay at all. I am going to come back to this interesting case in Section 4.5 below.

Another difficult problem is the arithmetic of rotation numbers r_b of the critical border curves. In Ref. [22] it was conjectured that the set of r_b consists of all combinations of only two elements $m=1$ and 2 in the continued fraction representation. This is sufficient for r_b to be random, and hence to explain irregular oscillations of the local exponent in the distribution of Poincaré recurrences (Section 3.1). This conjecture was partially confirmed numerically in Ref. [45]. Our recent refined conjecture is that r_b are the so-called Markov numbers [30].

4.4. Internal borders. Typically, the central part of principal critical resonances is not destroyed (see, e. g., Fig. 5). Hence, in any neighborhood of the main chaos border there is an infinite set of internal chaos borders, each one with its own critical structure. Assuming universality of critical phenomena at any chaos border we arrive at the following estimate in scaled variables

$$(\mu_q q^2)\sim\left(\frac{\tau}{q}\right)^{-p_c} \tag{4.9}$$

for a principal resonance q where μ_q is the sticking measure at the internal border.

The main difficulty here is in that the internal border exists not only inside the principal resonances but also in many others, near the critical border curve, which are not destroyed by the local supercritical perturbation. To estimate the total number of such resonances we can make use of Eq. (3.19) which determines the stability zone $\Delta K_s\sim\rho_s\sim q^{-1}$ for any q (as a very crude approximation, of course). Then, for a given q only $M_q/q\sim 1$ resonances fall into this zone, where $M_q\sim q$ is the total number of resonances p/q for a fixed q. Again, as a crude approximation we can extend the estimates, particularly Eq. (4.9), on all undestroyed resonances. As a result, the total internal border contribution to the correlation is

$$\tilde{C}_y\sim\sum_q \mu_q\sim\tau^{-p_c}\sum_q^{\tau} q^{p_c-2}, \tag{4.10}$$

where the sum is taken over all q up to τ. This contribution is essential if $p_c\geqslant 1$. But for $p_c>1$ the above estimate is not self-consistent as $\tilde{C}_y\sim\tau^{-1}$ contrary to assumed universality. However, the latter holds for $p_c=1$ (to logaritmic accuracy). This was the preliminary conclusion in Ref. [41] which was confirmed also in Ref. [42].

It would be a nice solution in the spirit of universality of the critical phenomena. Yet, first, the value $p_c=1$ seems still to be incompatible with numerical data (Section 3.1), and second, there is another possibility missed in Ref. [41], namely, $p_c<1$ as is suggested by numerical data. Then, the effect of internal borders is not decisive, at least, for exponent p_c whose value is determined by another mechanism, for example, one described in the previous Section.

In higher dimensions we have instead of Eq. (4.9) (see Section 3.5)

$$(\mu_q q^N)\sim\left(\frac{\tau}{q^{N-1}}\right)^{-p_c}. \tag{4.11}$$

In calculating the total contribution of all internal borders we need to take into account that now there are as many as $\sim q^{N-2}$ undestroyed resonances, for a given q, within the stability zone. Hence, the total «internal» correlation

$$\tilde{C}_y\sim\sum_q \mu_q q^{N-2}\sim\tau^{-p_c}\sum_q^{\tau^{1/(N-1)}} q^{p_c(N-1)-2}. \tag{4.12}$$

The critical value p_c^* of the critical exponent is $p_c^*=(N-1)^{-1}$. Only this value preserves universality based entirely on the internal borders. And, again, there is another possibility that $p_c<p_c^*$ so that internal borders are irrelevant. This is just the case if the above estimate (4.8) is true: $p_c=p_c^*/2$.

Preliminary numerical results obtained in collaboration with V.V. Vecheslavov ($p_c\approx 0.26$ and 0.19 for $N=3$ and 4, respectively) seem to confirm (or, at least, do not contradict) prediction (4.8).

4.5. Superfast diffusion [22]. Slow correlation decay with $p_c<1$ (4.5) may result in a superfast diffusion. Indeed, if this correlation determines the diffusion, the rate

$$D_z\sim\int C_y(\tau)\,d\tau$$

formally diverges. Here the diffusion goes in a new variable z, and $\dot{z}=y$. The divergence means that the dispersion (the second moment of the distribution function)

$$\sigma^2 \sim \int D\, d\tau \sim t^{2-p_c} \tag{4.13}$$

grows faster than time t. Hence the term «superfast diffusion» we use. This phenomenon was studied from different points of view in many papers (see, e. g., Refs [43, 44]).

The simplest example is again standard map for special values of parameter $K \approx 2\pi m$ with any integer $m \neq 0$. At these K the so-called accelerator modes exist [7] that is relatively small areas of regular motion with linearly increasing momentum: $y \sim \pm t$ while phase x is fixed. A chaotic trajectory cannot penetrate into these domains but it sticks at their borders. As a result, a superfast diffusion in y occurs which was first observed numerically in Ref. [46]. Notice that in the above notation $z=y$ now while the role of y plays a new coordinate normal to the chaos border surrounding the regular regions. According to Eq. (4.13)

$$\sigma^2 \approx \alpha \mu_s \frac{K^2}{2} t^{3/2} \sim t^{3/2}, \tag{4.14}$$

where $\alpha \approx 0.5$ from numerical data [46] for $K \approx 2\pi$, and relative stable area $\mu_s \approx 0.02$. As $\mu_s \sim K^{-2}$ [7] the rate of this anomalous diffusion ($\sigma^2/t^{3/2}$) does not depend either on $K \to \infty$ or on $\mu_s \to 0$.

In Ref. [44, 47] more complicated accelerator modes were shown to produce a superfast diffusion also corresponding to $p_c \approx 2/3$ in reasonable agreement with our numerical data. A simple expression for the growth of all moments of the distribution function was also given in Ref. [44], namely:

$$\sigma^k \sim t^{k-p_c} \tag{4.15}$$

for k even. In higher dimensions when $N \to \infty$, and $p_c \to 0$ this relation becomes especially simple but somewhat puzzling. It appears to describe almost a free motion but in both directions of z variable! The limiting case $p_c=0$ corresponds to the fastest homogeneous diffusion possible.

Further insight into the nature of superfast diffusion can be obtained from the motion power spectrum which is the Fourier transform of the correlation [30]. For $\omega \to 0$ we have from Eq. (4.8)

$$S_y(\omega) \sim \omega^{p_c-1} \sim \omega^{-\frac{2N-3}{2N-2}}. \tag{4.16}$$

As $N \to \infty$ it approaches the famous $1/\omega$ spectrum which, thus, produces the fastest diffusion. If $\dot{z}=y$, the spectrum of z-motion is

$$S_z = \frac{S_y}{\omega^2} \sim \omega^{p_c-3}. \tag{4.17}$$

From normalization (Parseval theorem)

$$\overline{z^2} = \int S_z(\omega)\, d\omega \sim \omega^{p_c-2} \sim t^{2-p_c}. \tag{4.18}$$

If $p_c<1$ the integral diverges as $\omega \to 0$. For a finite time interval the minimal $\omega \sim t^{-1}$, and the diffusion law (4.13) is recovered, including the limiting $p_c=0$. However, in the latter case the velocity dispersion $\overline{y^2} \sim \ln \omega$ diverges (see Eq. (4.16)). In our models with a chaos border this is impossible, hence, always $p_c > 0$ (4.8).

The theory of superfast diffusion can be applied to a broad variety of different problems. A nice example is the tangle of a long polymeric molecule in a certain environment. Approximately, such a molecule can be considered as a trajectory of the self-avoiding random walk. The constraint imposes a long-term correlation which can be estimated as follows. Suppose that the molecule length l and the tangle size σ are related by

$$\sigma^2 \sim l^{2\nu} \tag{4.19}$$

with some so far unknown parameter ν. Then, the correlation due to avoided crossings of molecule line is roughly proportional to the probability of the self-crossing:

$$C \sim \frac{l}{\sigma^d} \sim l^{1-\nu d}, \tag{4.20}$$

where integer d is the space dimensions. Hence, we have a power-law correlation with the exponent $p_c = \nu d - 1$. Using Eq. (4.13) with $t=l$ and Eq. (4.19) we arrive at the relation

$$2\nu = 3 - \nu d; \quad \nu = \frac{3}{2+d}, \tag{4.21}$$

which is known as Flory formula (see, e. g., Ref. [48]). It was derived in a completely different way (from the thermodynamics of

a polymeric molecule), and holds for $d \leqslant 4$, otherwise $\nu = 1/2$. In our dynamical approach the latter limitation follows from the condition $p_c < 1$ for anomalous diffusion. In the border case $\sigma^2 \sim l \ln l$ (see, e. g., T. Geisel et al in Ref. [43]) which slightly differs from Flory formula.

4.6. Fractal properties [49]. The critical structure in Hamiltonian systems is also called «random fractals» (R. Voss, Ref. [43]) because of the renormchaos (Section 3.4) or «fat fractals» [49] for their finite measure unlike dissipative systems. Some fractal properties were studied numerically in Ref. [49].

Here I am going to explain one property — the fractal dimension d_L of the set of all chaos borders (mainly internal ones, of course). It is inferred from the dependence of the measure μ_{ch} of a chaotic component on spatial linear resolution $\varepsilon \to 0$:

$$\mu_{ch}(\varepsilon) = \mu_{ch}(0) + \alpha \varepsilon^{\beta}. \tag{4.22}$$

Here $\mu_{ch}(0) > 0$ is the measure of the whole chaotic component, hence, its dimension $d_S = 2$ is topological. The second term represents the borders whose total length and dimension are

$$L(\varepsilon) \sim \varepsilon^{\beta - 1}; \quad d_L = 2 - \beta. \tag{4.23}$$

The simplest evaluation of this scaling can be done as follows (see Section 4.4). Each undestroyed resonance has internal borders of the total length $l_q \sim 1$. This estimate follows from the fact that an individual border is a nonfractal curve whose dimension $d_l = 1$ is topological. It is because the ratio of transverse to longitudinal scaling factors of the critical structure $s_b/s_a = q_n \to \infty$ as $n \to \infty$ (see Sections 3.2 and 3.3). Thus, the border curve $y_b(x)$ is very smooth (see Fig. 5). The number of undestroyed resonances is of the order of maximal $q = q_{\max}$ which is determined by the resolution: $\varepsilon \sim q_{\max}^{-2}$. Hence

$$L \sim \varepsilon^{-1/2}; \quad \beta = \frac{1}{2}; \quad d_L = \frac{3}{2} \tag{4.24}$$

in a reasonable agreement with numerical $\beta = 0.3 - 0.7$ [49].

Notice also that the total number of resolved borders scales, in this approximation, as

$$N_b \sim q_{\max}^2 \sim \varepsilon^{-1}. \tag{4.25}$$

In higher dimensions with N frequencies we need to consider N-dimensional map with nonfractal border surfaces of $N-1$ dimensions. Now there are $\sim q^{N-1}$ undestroyed resonances up to $q_{\max} \sim \varepsilon^{-1/N}$. The border surface in each such resonance $S_1 \sim 1$, and total border surface and its dimension are

$$S_b \sim \varepsilon^{\left(1 - \frac{1}{N}\right)}; \quad d_S = N - \frac{1}{N}. \tag{4.26}$$

The total number of resolved border surfaces, or of the domains with regular motion

$$N_b \sim \varepsilon^{-1} \tag{4.27}$$

does not depend on N, and in this sense is universal.

Acknowledgements. I would like to express my sincere gratitude to D.L. Shepelyansky, my main collaborator in the studies of critical phenomena, to F. Vivaldi who attracted our attention to this interesting problem, and to G. Casati, D. Escande, R. MacKay, I. Percival and Ya. G. Sinai for stimulating discussions.

REFERENCES

1. *V.M. Alekseev and M.V. Yakobson.* Rhys. Reports, **75** (1981) 287.
2. *G. Chaitin.* Information, Randomness and Incompleteness, World Scientific, 1990.
3. *B.V. Chirikov, F.M. Izrailev and D.L. Shepelyansky.* Physica, D **33** (1988) 77.
4. *B.V. Chirikov.* Time-Dependent Quantum Systems, Proc. Les Houches Summer School on Chaos and Quantum Physics, Elsevier, 1990.
5. *A. Lichtenberg, M. Lieberman.* Regular and Stochastic Motion, Springer, 1983.
6. *G.M. Zaslavsky.* Chaos in Dynamic Systems, Harwood, 1985.
7. *B.V. Chirikov.* Phys. Reports, **52** (1979) 263.
8. *B.V. Chirikov and V.V. Vecheslavov.* Astron. Astroph., **221** (1989) 146.
9. *G. Casati et al.* Phys. Rev., A **36** (1987) 3501.
10. *A.A. Chernikov, R.Z. Sagdeev and G.M. Zaslavsky.* Physica, D **33** (1988) 65.
11. *B.V. Chirikov.* Foundations of Physics, **16** (1986) 39.
12. *M. Eisenman et al.* Lecture Notes in Physics, **38** (1975) 112; *J. von Hemmen.* Ibid, **93** (1979) 232.
13. *B.G. Konopelchenko.* Nonlinear Integrable Equations, Lecture Notes in Physics, **270** (1987).
14. *B.V. Chirikov and V.V. Vecheslavov.* KAM Integrability. — In: Analysis etc., Academic Press, 1990, p.219.
15. *V.I. Arnold and A. Avez.* Ergodic Problems in Classical Mechanics, Benjamin, 1968.
16. *B.V. Chirikov.* Proc. Roy. Soc. Lond., A **413** (1987) 145.
17. *A. Rechester et al.* Phys. Rev., A **23** (1981) 2664.
18. *B.V. Chirikov, D.L. Shepelyansky.* Radiofizika, **29** (1986) 1041.

19. *F. Vivaldi.* Private communication.
20. *I. Kornfeld, S. Fomin and Ya. Sinai.* Ergodic Theory, Springer, 1982.
21. *R. MacKay.* Physica, D **7** (1983) 283.
22. *B.V. Chirikov and D.L. Shepelyansky.* Physica, D **13** (1984) 395.
23. *R. Artuso, G. Casati and D.L. Shepelyansky.* Breakdown of Universality in Renormalization Dynamics for Critical Invariant Torus, Phys. Rev. Lett. (to appear).
24. *B.V. Chirikov, D.L Shepelyansky.* Proc. 9th Int. Conf. on Nonlinear Oscillations (Kiev, 1981). Kiev, Naukova Dumka, 1983, v. 2, p.421. English translation available as preprint PPL-TRANS-133, Plasma Physics Lab., Princeton Univ., 1983.
25. *S. Channon and J. Lebowitz.* Ann. N. Y. Acad. Sci., **357** (1980) 108.
26. *G. Paladin and A. Vulpiani.* Phys. Reports, **156** (1987) 147.
27. *C. Karney.* Physica, D *8* (1983) 360.
28. *P. Grassberger and I. Procaccia.* Physica, D **13** (1984) 34.
29. *J. Bene, P. Szèpfalusy and A. Fülöp.* A Generic Dynamical Phase Transition in Chaotic Hamiltonian Systems, Phys. Rev. Lett. (to appear).
30. *B.V. Chirikov and D.L. Shepelyansky.* Chaos Border and Statistical Anomalies. — In: Renormalization Group/D.V. Shirkov, D.I. Kazakov and A.A. Vladimirov Eds., World Scientific, Singapore, 1988, p.221.
31. *B.V. Chirikov.* Intrinsic Stochasticity, Proc. Int. Conf. on Plasma Physics, Lausanne, 1984, v.2, p.761.
32. *G. Schmidt and J. Bialek.* Physica, D **5** (1982) 397.
33. *J. Greene, J. Math.* Phys., **9 (1968) 760; 20** (1979) 1183.
34. *M. Feigenbaum, J. Stat.* Phys., **19** (1978) 25; **21** (1979) 669.
35. *S. Ostlund et al.* Physica, D **8** (1983) 303.
36. *E.M. Lifshits et al.* Zh. Eksp. Teor. Fiz., **59** (1970) 322; ibid (Pisma), **38** (1983) 79.
    J. Barrow, Phys. Reports, **85** (1982) 1.
37. *B.V. Chirikov.* The Nature and Properties of the Dynamic Chaos, Proc. 2d Int. Seminar «Group Theory Methods in Physics» (Zvenigorod, 1982), Harwood, 1985, v.1, p.553.
38. *I. Dana et al.* Phys. Rev. Lett., **62** (1989) 233.
39. *R. MacKay et al.* Physica, D **13** (1984) 55.
40. *J. Hanson et al.* J. Stat. Phys., **39** (1985) 327.
41. *B.V. Chirikov.* Lecture Notes in Physics, **179** (1983) 29.
42. *J. Meiss and E. Ott.* Phys. Rev. Lett., **55** (1985) 2741; Physica, D **20** (1986) 387.
43. *P. Lévy.* Théorie de l'addition des variables eléatoires, Gauthier-Villiers, Paris, 1937.
    T. Geisel et al. Phys. Rev. Lett. **54** (1985) 616;
    R. Pasmanter. Fluid Dynamic Research, **3** (1988) 320.
    R. Voss. Physica, D **38** (1989) 362.
    G. M. Zaslavsky et al. Zh. Exper. Teor. Fiz., **96** (1989) 1563.
44. *H. Mori et al.* Prog. Theor. Phys. Suppl., 1989, N 99, p.1.
45. *J. Greene et al.* Physica, D **21** (1986) 267.
46. *C. Karney et al.* Ibid, **4** (1982) 425.
47. *Y. Ichikawa et al.* Ibid, **29** (1987) 247.
48. *P. de Gennes.* Scaling Concepts in Polymer Physics, Cornell Univ. Press., 1979.
49. *D. Umberger and D. Farmer.* Phys. Rev. Lett. **55** (1985) 661.
    C. Grebogi et al. Phys. Lett., A **110** (1985) 1.

Boris V. Chirikov

Patterns in Chaos

Б.В. Чириков

Структура хаоса

Ответственный за выпуск С.Г.Попов

Работа поступила 14 сентября 1990 г.
Подписано в печать 14.09 1990 г.
Формат бумаги 60×90 1/16 Объем 3,0 печ.л., 2,6 уч.-изд.л.
Тираж 290 экз. Бесплатно. Заказ № 109.

Набрано в автоматизированной системе на базе фотонаборного автомата ФА1000 и ЭВМ «Электроника» и отпечатано на ротапринте Института ядерной физики СО АН СССР,
Новосибирск, 630090, пр. академика Лаврентьева, 11.